Available online at www.sciencedirect.com

SCIENCE DIRECT®

Magnetic Resonance Imaging 23 (2005) 953–959

MAGNETIC RESONANCE IMAGING

Implications of the Rician distribution for fMRI generalized likelihood ratio tests

Arnold J. den Dekker[a,1], Jan Sijbers[b,*]

[a]Delft Center for Systems and Control, Delft University of Technology, 2628 CD Delft, The Netherlands
[b]Vision Laboratory, CMI, University of Antwerp, B-2020 Antwerpen, Belgium

Received 16 December 2004; accepted 6 July 2005

Abstract

In functional magnetic resonance imaging (fMRI), the general linear model test (GLMT) is widely used for brain activation detection. However, the GLMT relies on the assumption that the noise corrupting the data is Gaussian distributed. Because the majority of fMRI studies employ magnitude image reconstructions, which are Rician distributed, this assumption is invalid and has significant consequences in case the signal-to-noise ratio (SNR) is low. In this study, we show that the GLMT should not be used at low SNR. Furthermore, we propose a generalized likelihood ratio test for magnitude MR data that has the same performance compared to the GLMT for high SNR, but performs significantly better than the GLMT for low SNR.

Keywords: fMRI; Statistical parametric maps; Generalized likelihood ratio test

1. Introduction

Functional magnetic resonance imaging (fMRI) is a well-known imaging technique to visualize functional activity in the human brain. The aim of fMRI is to determine regions in the brain that show significant neural activity upon stimulus presentation by statistically analyzing a sequence of MR brain images acquired over time. In the past, many statistical tests have been proposed for the construction of statistical parametric maps (see, e.g., Ref. [1] for an overview). Most of these tests are applied to magnitude MR images, because magnitude images have the advantage to be immune to incidental phase variations due to various sources. However, because magnitude images are obtained by computing the magnitude of complex valued, Gaussian-distributed images, they are known to be Rician distributed [2,3]. Nevertheless, standard tests based on magnitude data generally rely on the assumption that these data are Gaussian distributed, which is a valid assumption only when the signal-to-noise ratio (SNR) is high. However, by pursuing fMRI image data with a sufficient SNR, spatial resolution is generally compromised. Therefore, it is of great interest to develop reliable methods that would work also on low SNR fMRI data to detect small intensity variations generated by neural activation [4]. This would allow to correctly process fMRI series with higher spatial resolution or fMRI images with a large degree of signal dropout [5].

In the past few years, generalized likelihood ratio tests (GLRTs) were developed to account for low SNR fMRI data [5–7]. These tests are based on complex valued data in which the phase in each voxel is described by a constant phase model [5,6] or a general linear model [7]. However, it has recently been shown that GLRTs based on complex valued data are very sensitive to (even small) errors in the phase model [8]. Moreover, for an increasing number of parameters in the phase model, the detection rate of those GLRTs drops drastically. Hence, tests based on magnitude data instead of complex valued data are likely to perform better, at least if the correct probability density function (PDF) of the data is taken into account [8].

The most popular test currently applied to fMRI data is the general linear model test (GLMT) [9]. The GLMT is in fact a GLRT under the assumption of Gaussian-distributed noise. It is to be expected that the performance of the test

* Corresponding author. Tel.: +32 3 265 34 52; fax: +32 3 265 33 18.
E-mail addresses: a.j.dendekker@dcsc.tudelft.nl (A.J. den Dekker), jan.sijbers@ua.ac.be (J. Sijbers).
[1] Tel.: +31 15 278 18 23; fax: +31 15 278 66 79.

0730-725X/$ – see front matter © 2005 Elsevier Inc. All rights reserved.
doi:10.1016/j.mri.2005.07.008

will suffer from the inaccuracy of the Gaussian approximation (especially for low SNR). In this paper, an alternative GLRT is proposed, which fully exploits the knowledge of the Rician distribution of the magnitude data and is therefore expected to be more reliable.

The paper starts with a brief review of the general theory for the construction of a GLRT. Next, the theory is applied to derive the GLMT as well as the GLRT for magnitude MR data that fully exploits the knowledge of the Rician distribution. The performance of this GLRT is compared to that of the GLMT. In this way, the sensitivity of the GLMT to the non-Gaussian distribution of the magnitude data is evaluated.

2. A general description of GLRTs

Let $\underline{\boldsymbol{m}}=(\underline{m}_1,\ldots,\underline{m}_N)^T$ be an $N\times 1$ random sample vector with joint PDF $p_{\underline{\boldsymbol{m}}}(\boldsymbol{x};\theta)$, in which $\theta=(\theta_1,\ldots,\theta_k)^T$ denotes the vector of unknown parameters and $\boldsymbol{x}=(x_1,\ldots,x_N)^T$ represents the vector of variables corresponding to the random sample vector $\underline{\boldsymbol{m}}$[2]. Suppose that we wish to test the composite null hypothesis:

$$H_0:\theta_1=\theta_1^0,\cdots,\theta_r=\theta_r^0,\theta_{r+1},\cdots,\theta_k \tag{1}$$

where $\theta_1^0,\ldots,\theta_r^0$ are known and $\theta_{r+1},\ldots,\theta_k$ are left unspecified against the alternative composite hypothesis H_1 under which all parameters $\theta_1,\ldots,\theta_k$ are left unspecified.

Next, consider a set of observations $\boldsymbol{m}=(m_1,\ldots,m_N)T$, and suppose that we substitute these observations for the corresponding variables $\boldsymbol{x}$ in the joint PDF of $\underline{\boldsymbol{m}}$. The resulting function is the so-called likelihood function $L(\theta;\boldsymbol{m})$. Then the generalized likelihood ratio (GLR) λ is defined as [10]:

$$\lambda\equiv\lambda(\boldsymbol{m})=\frac{\sup\limits_{\theta_1,\cdots,\theta_k} L(\theta_1,\cdots,\theta_k;\boldsymbol{m})}{\sup\limits_{\theta_{r+1},\cdots,\theta_k} L(\theta_1^0,\cdots,\theta_r^0,\theta_{r+1},\cdots,\theta_k;\boldsymbol{m})} \tag{2}$$

The denominator of λ is the likelihood function evaluated at the maximum likelihood (ML) estimates of the unknown parameters under H_0, whereas the numerator is the likelihood function evaluated at the ML estimates of the unknown parameters under H_1. Note that λ is a function of the observations $\boldsymbol{m}$ only. If these observations are replaced by their corresponding random variables $\underline{\boldsymbol{m}}$, then we write $\underline{\lambda}$ for λ. The GLRT principle now states that H_0 is to be rejected if and only if the sample value λ of $\underline{\lambda}$ satisfies the inequality $\lambda\geq\lambda_0$ where λ_0 is some user-specified threshold.

[2] In what follows, random variables are underlined, small bold characters denote vectors and capital bold characters denote matrices. The superscript T denotes matrix transposition.

It can be shown that, asymptotically (i.e., for $N\to\infty$), the modified GLR statistic $2\ln\underline{\lambda}$ possesses a χ_r^2 distribution, that is, a χ^2 distribution with r degrees of freedom, when H_0 is true [11,12]. If the model is linear in the parameters and the noise is Gaussian distributed, this not only holds asymptotically, but also for a finite number of observations. Knowledge of the statistic's PDF allows one to compose GLRTs with a desired *false alarm rate*. The false alarm rate P_f is defined as the probability that the test will decide H_1 when H_0 is true. The false alarm rate is also known as the significance level of the test [12]. The *detection rate* P_d is defined as the probability that the test will decide H_1 when H_1 is true. Furthermore, a test has the so-called constant false alarm rate (CFAR) property if the threshold required to maintain a constant P_f can be found independent of the SNR, which is usually unknown beforehand. As follows from above, GLRTs will have the CFAR property at least asymptotically.

3. Generalized likelihood ratio tests for magnitude fMRI data

In this section, we apply the theory described in the previous section to construct GLRTs for functional magnitude MR data. Thereby, we will consider the problem of testing whether the response of a magnitude MR data set $\boldsymbol{m}=(m_1,\ldots,m_N)^T$ of sample size N to a known reference function $\boldsymbol{r}=(r_1,\ldots,r_N)^T$ is significant. Thereby, the noiseless magnitude data set is assumed to be described by the following $N\times 1$ deterministic signal vector:

$$\boldsymbol{z}=a\mathbf{1}+b\boldsymbol{r} \tag{3}$$

with $\mathbf{1}$ an $N\times 1$ vector of ones. Hence, $\boldsymbol{z}$ is a constant baseline on which a reference function $\boldsymbol{r}$ with amplitude b is superimposed. In the absence of activity, $b=0$, so that $\boldsymbol{z}\equiv a\mathbf{1}$. We will consider the problem of testing the hypothesis that $b=0$ (H_0) against the hypothesis that $b\neq 0$ (H_1).

In what follows, to simplify the discussion, it will be assumed that the noise variance σ^2 is known. This is usually a valid assumption, because the noise variance can mostly be estimated independently with high accuracy and precision [13,14]. In Section 3.1, we will derive a GLRT based on the assumption of Gaussian-distributed data, which will lead to the well-known GLMT. Next, in Section 3.2, we will derive a new GLRT based on Rician-distributed data.

3.1. Generalized likelihood ratio test based on Gaussian-distributed data

In what follows, it is assumed that the magnitude data can be described as

$$\underline{\boldsymbol{m}}=\boldsymbol{z}+\underline{\boldsymbol{e}} \tag{4}$$

with $\underline{\boldsymbol{e}}$ an $N\times 1$ vector of which the components are zero mean, Gaussian-distributed noise with variance σ^2. Under

this assumption, the likelihood function of the data is given by

$$L(\boldsymbol{z};\boldsymbol{m}) = \left(\frac{1}{2\pi\sigma^2}\right)^{\frac{N}{2}} \mathrm{e}^{-\frac{1}{2\sigma^2}||\boldsymbol{m}-\boldsymbol{z}||^2} \tag{5}$$

Closed form expressions for the maximum likelihood estimators (MLEs) of the unspecified parameters can easily be derived [15].

Under H_0, in which $\boldsymbol{z}=a\mathbf{1}$, the MLE $\underline{\hat{a}}_0$ of the parameter a is given by

$$\underline{\hat{a}}_0 = \frac{1}{N}\underline{\boldsymbol{m}}^T.\mathbf{1} \tag{6}$$

Under H_1, in which $\boldsymbol{z}=a\mathbf{1}+b\boldsymbol{r}$, the MLEs $\underline{\hat{a}}_1$ and $\underline{\hat{b}}$ of the parameters a and b are given by

$$\begin{pmatrix} \underline{\hat{a}}_1 \\ \underline{\hat{b}} \end{pmatrix} = \left(\boldsymbol{X}^T\boldsymbol{X}\right)^{-1}\boldsymbol{X}^T\underline{\boldsymbol{m}} \tag{7}$$

with $\boldsymbol{X}$ an $N\times 2$ matrix given by $\boldsymbol{X}=(\mathbf{1}\ \boldsymbol{r})$.

From Eqs. (2) and (5), and using Eqs. (6) and (7), a closed form expression for the modified GLR statistic can be obtained:

$$2\ln\underline{\lambda} = \frac{1}{\sigma^2}\left[||\underline{\boldsymbol{m}} - \underline{\hat{a}}_0\mathbf{1}||^2 - ||\underline{\boldsymbol{m}} - \underline{\hat{a}}_1 - \underline{\hat{b}}\boldsymbol{r}||^2\right] \tag{8}$$

It can be shown that Eq. (8) will possess an χ_1^2 distribution under H_0 [16]. This allows one to select a proper threshold so as to achieve a desired false alarm rate. Moreover, this means that under the assumption of Gaussian-distributed data, the test under concern will possess the CFAR property. In what follows, the test described in this subsection will be called the GLMT.

3.2. Generalized likelihood ratio test based on Rician-distributed data

Next, we will no longer assume that the magnitude data are Gaussian distributed. Instead, we will exploit the fact that we know that the magnitude data are Rician distributed. The Rician PDF of magnitude data with deterministic signal component z and noise variance σ^2 is given by [2]

$$p_{\underline{m}}(x|z) = \frac{x}{\sigma^2}\mathrm{e}^{-\frac{x^2+z^2}{2\sigma^2}} I_0\left(\frac{zx}{\sigma^2}\right)\epsilon(x) \tag{9}$$

where I_0 is the zeroth order modified Bessel function of the first kind. The unit step Heaviside function $\varepsilon(.)$ is used to indicate that the expression for the PDF of x is valid for nonnegative values of x only. Then, the likelihood functions for the Rician-distributed data under H_0 and H_1 are given by

$$L(a;\boldsymbol{m}) = \prod_{n=1}^{N} \frac{m_n}{\sigma^2}\mathrm{e}^{-\frac{m_n^2+a^2}{2\sigma^2}} I_0\left(\frac{m_n a}{\sigma^2}\right) \tag{10}$$

$$L(a,b;\boldsymbol{m}) = \prod_{n=1}^{N} \frac{m_n}{\sigma^2}\mathrm{e}^{-\frac{m_n^2+(a+br_n)^2}{2\sigma^2}} I_0\left(\frac{m_n(a+br_n)}{\sigma^2}\right) \tag{11}$$

respectively, and the likelihood ratio test statistic is given by

$$\underline{\lambda} = \frac{\sup\limits_{a,b} L(a,b;\underline{\boldsymbol{m}})}{\sup\limits_{a} L(a;\underline{\boldsymbol{m}})} \tag{12}$$

The modified test statistic 2 ln $\underline{\lambda}$ is then asymptotically χ_1^2 distributed under H_0. Unfortunately, no closed form expression for the test statistic [Eq. (12)] can be derived. Hence, $\underline{\lambda}$ is found by numerical optimization.

4. Simulation results and discussion

Monte Carlo simulation experiments were set up to evaluate the performance of the GLMT and the Rician PDF-based GLRT. For this purpose, numerous realizations of N Rician-distributed magnitude time series were generated of which the deterministic signal components are described by Eq. (3).

In the majority of reported functional human brain mapping studies using fMRI, blocks of rest and activation images are scanned periodically. Typically, a number of frames are acquired while the subject is at rest or under some baseline condition. This is followed by a number of activation frames during which the subject is receiving a sensory stimulus or performing a specified motor or cognitive task. This pattern is then repeated for a number of cycles. The activation-baseline pattern can be represented by a periodic rectangular waveform with values of +1 and −1 representing activation and baseline conditions, respectively [17]. For this reason, for the sake of simplicity, a square wave was chosen as a reference function in our experiments. Note, however, that the theory presented in this paper, as well as the conclusions drawn therefrom, easily generalize to an arbitrary reference function.

In our simulation experiments, the reference function $\boldsymbol{r}$, as given in Eq. (3), was chosen to be a square wave fluctuating between −1 and +1 with period 20. The true baseline parameter a was fixed to 10. The true parameter b of the reference function r was fixed to 1. The standard deviation σ of the noise was varied from 0.1 to 10. Hence, the average SNR of the fMRI time series, defined as a/σ, ranged from 100 to 1. For each set of parameters, the CFAR property as well as the detection rates of the tests described above was evaluated, which will be described in Sections 4.1 and 4.2, respectively. For numerical optimization, while running the GLRT test, the routine *Amoeba* from Numerical Recipes was employed [18].

4.1. CFAR property

First, simulation experiments have been conducted so as to find out to what extent the tests under concern have the CFAR property, that is, whether a specified false alarm rate P_f could be achieved irrespective of the SNR. The reason for this is that tests that do not have the CFAR property are of little practical use, because the SNR is unknown

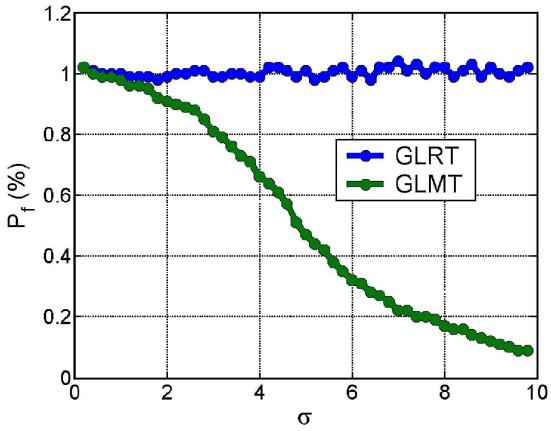

Fig. 1. For $N=120$ and $a=10$, the false alarm rate P_f is shown as a function of σ for the GLMT and the GLRT based on Rician-distributed data. For both tests, the threshold was set to $\chi^2_{1,0.99}$. Note that for the tests to have the CFAR property, the false alarm rate P_f should be 1%, irrespective of the SNR.

beforehand. Although it is known that the GLRT has the CFAR property asymptotically, it remains to be seen whether this property still applies to a finite number of observations. Moreover, the GLMT is based on the assumption of Gaussian-distributed data, which is an invalid assumption for magnitude data. Clearly, this may affect the CFAR property of the test.

To test the CFAR property, simulated fMRI null data sets were generated with no activation pattern (i.e., $b=0$) as a function of σ (i.e., the SNR because a is fixed). Next, the GLMT as well as the proposed GLRT was applied to the time series. Because no activation was presented, possible detected activations (due to the noise) were classified as false positives. In all experiments, the threshold of the test statistic was set as to obtain a false alarm rate P_f of 1%. If a test would have the CFAR property, a CFAR of 1% would be expected as a function of σ. The results of this experiment are shown in Fig. 1.

Simulation results revealed that for numbers of observations that are representative of those available in practical fMRI measurements, the GLRT based on the Rician distribution has the CFAR property, at least for SNR >1. The GLMT, on the other hand, loses its CFAR property for relatively low SNR values (SNR <10). This loss of the CFAR property of the GLRT was observed to be independent of N. For $N=120$, P_f is plotted as a function of σ for both tests in Fig. 1. For both tests, the threshold was set to $\chi^2_{1,0.99}$, that is, the 99% quantile of the χ^2_1 distribution. For each point, a sample size of 10^6 was employed.

Because of the lack of CFAR property of the GLMT at low values of the SNR, it is clear that the GLMT should never be used for low SNR fMRI time series. Indeed, if one would like to fix the false alarm rate at, for example, 1%,

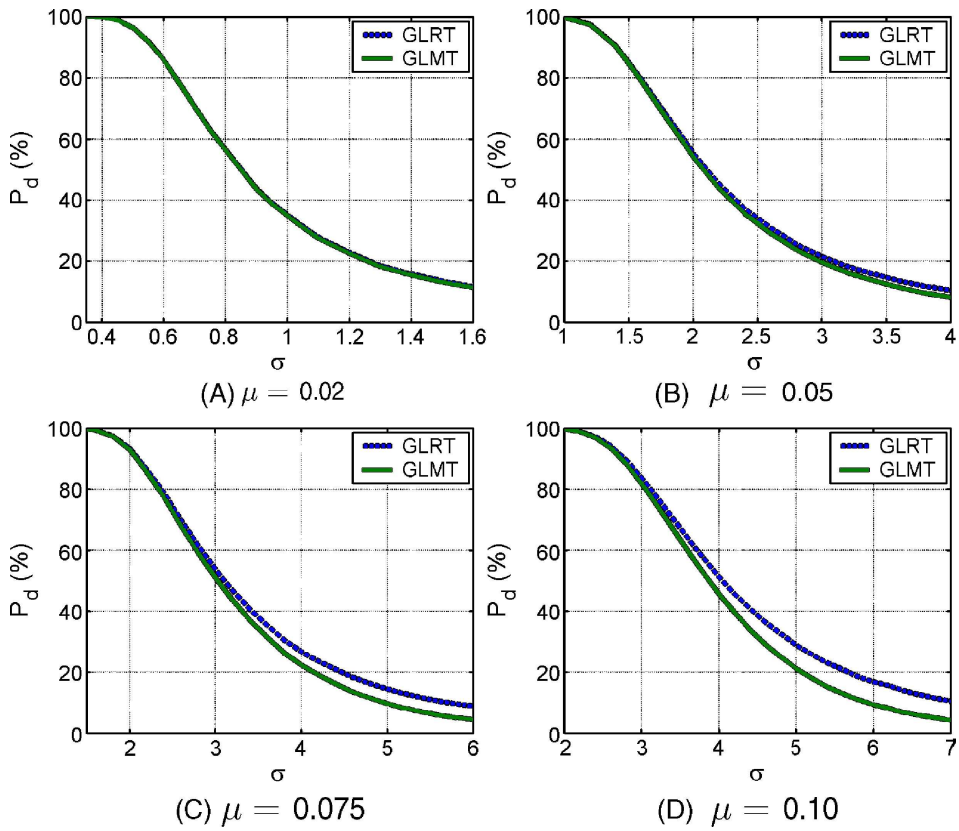

Fig. 2. For $N=120$, $a=10$ and $P_f=1\%$, the detection rates P_d are shown as a function of σ for the GLMT and the GLRT based on Rician-distributed data. Results are shown for three different values of the response strength μ, namely $\mu=0.02$ (A), $\mu=0.05$ (B), $\mu=0.075$ (C), and $\mu=0.10$ (D), respectively.

one is unable to set the proper threshold for the GLMT statistic to have a false alarm rate of 1%. This is because, in practice, the true SNR is unknown. In other words, at low SNR, the activations detected by the GLMT are meaningless because the false alarm rate with which the threshold set by the user corresponds with is unknown.

4.2. Detection rate

Next, simulation experiments were run in which, for a fixed false alarm rate, the detection rate P_d was determined as a function of the SNR (sample size was 10^5). This was done for several values of the relative response strength $\mu=b/a$, and for $N=120$. In each experiment, the threshold of both sets was set to $\chi^2_{1,0.99}$. For truly χ^2_1 distributed test statistics, this would lead to a false alarm rate $P_f=0.01$, which is a representative value of the P_f values used in fMRI.

The results obtained from the experiments showed that the detection rate P_d of the proposed GLRT is never smaller than those for the GLMT. For high values of the SNR, the detection rates do not differ significantly. For a decreasing value of the SNR, however, the difference in detection rate between the GLMT and the proposed GLRT increases. This is shown in Fig. 2.

In order to have a visual appreciation of the difference in detection rate, a simulation experiment was set up in which an fMRI time series was generated as follows. First, a synthetic, noiseless MRI image was generated using an MRI brain simulator, which resembles to some extent real MRI brain data (available from http://www.bic.mni.mcgill.ca/brainweb) [19]. For each voxel, an fMRI trace was generated using a similar activation curve as described in the first paragraphs of Section 4. Thereby, only in the three square zones activation was induced (see Fig. 3A) with $\mu=0.05$, $\mu=0.075$ and $\mu=0.10$. Finally, all fMRI traces were polluted with Rician-distributed noise with standard deviations $\sigma=2.5$, $\sigma=4.0$ and $\sigma=5.0$, respectively [20].

The differences in the parametric map for both the GLMT and the GLRT can be visually appreciated from Fig. 3. The first column of Fig. 3 shows three square activation regions. The second and third columns show the detection

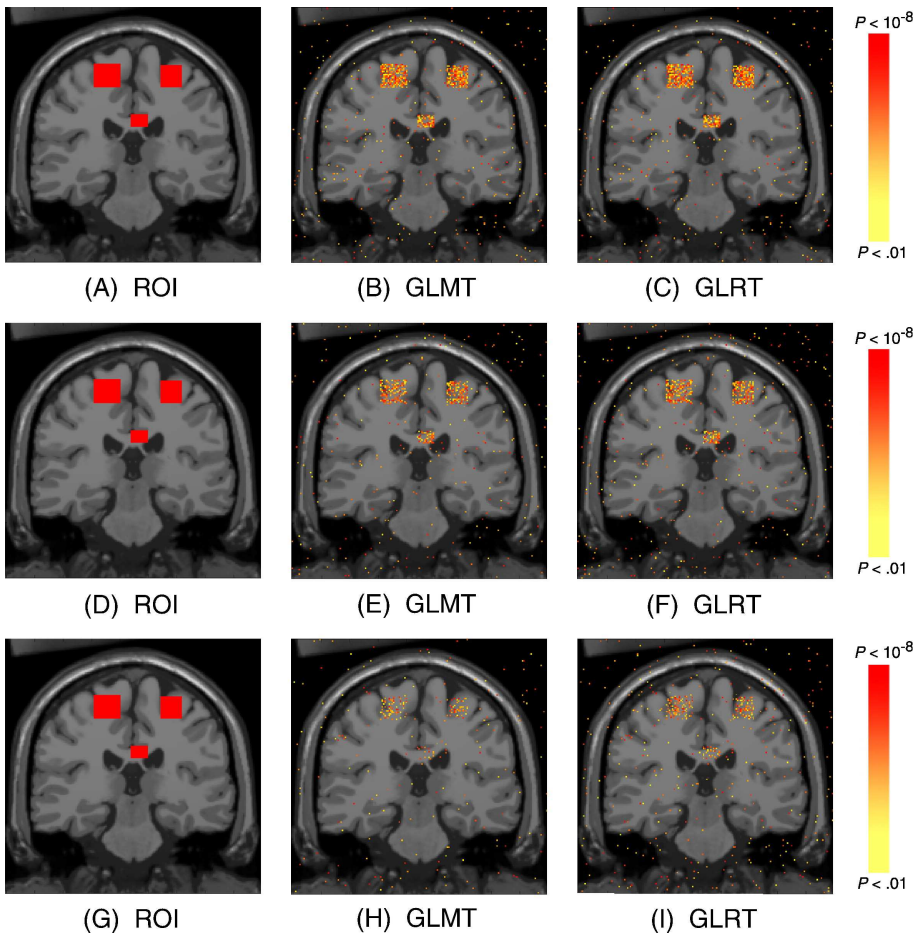

Fig. 3. Activation detection results of the GLMT and the proposed GLRT. Synthetic MRI images are shown with activations superimposed in color. The first column (A, D, G) shows three regions in which functional activation was simulated. The second column (B, E, H) and third column (C, F, I) show the detection results (in terms of P values) of the GLMT and the proposed GLRT, respectively. Activation detection is done at a false alarm rate of 0.01. This was done for three values of μ, 0.05, 0.075 and 0.10, shown in the first row (A–C), second row (D–F) and third row (G–I), respectively. The corresponding values of σ were 2.5, 4.0 and 5.0.

results of the GLMT and the GLRT, respectively. The relative response strength for the first, second and third row was $\mu=0.05$, $\mu=0.075$ and $\mu=0.10$, with $\sigma=2.5$, $\sigma=4.0$ and $\sigma=5.0$, respectively. The results are shown in terms of the so-called P values produced by both tests. The P value is defined as the probability that the test statistic would assume a value greater than or equal to the observed value under the assumption that H_0 (no activation) is true [21]. In other words, the P value is the smallest significance level at which the null hypothesis would be rejected for the set of observations. A small P value provides strong evidence against the null hypothesis. In Fig. 3, the P values of activated voxels are shown, where a voxel was labeled as activated if it had a P value below 0.01. This means that the P values shown range from 8.0 to 0.01. Red colors represent stronger evidence against the null hypothesis (i.e., smaller P values), as indicated by the color bar.

In order to generate a better impression of the detection rate difference, a simple clustering scheme was applied to the images shown in Fig. 3, of which the results are shown in Fig. 4. Thereby, a voxel was assigned the average of the P values from activated voxels within a 5×5 neighborhood if the number of activated voxels within that neighborhood exceeded a specified threshold (chosen to be 9). This clustering enhances the detection of activated areas and removes the false positives. From the figure, it is clear that when the SNR is relatively high, the detection rates of the GLMT and the GLRT are comparable. However, with decreasing values of the SNR, the detection rate of the proposed GLRT is significantly better than that of the GLMT.

At this point, it has to be emphasized again that in order to compare detection rates in a fair way, the false alarm rate of the tests under concern should be equal. As is clear from Section 4.1, this is not the case because the GLMT lacks the CFAR property, and therefore, the detection rates of both tests should be interpreted with care. Nevertheless, the results in Figs. 2–4 visualize what the detection rates would be for the GLMT and the GLRT if the commonly assumed χ^2_1 distribution under H_0 is employed. It was observed from

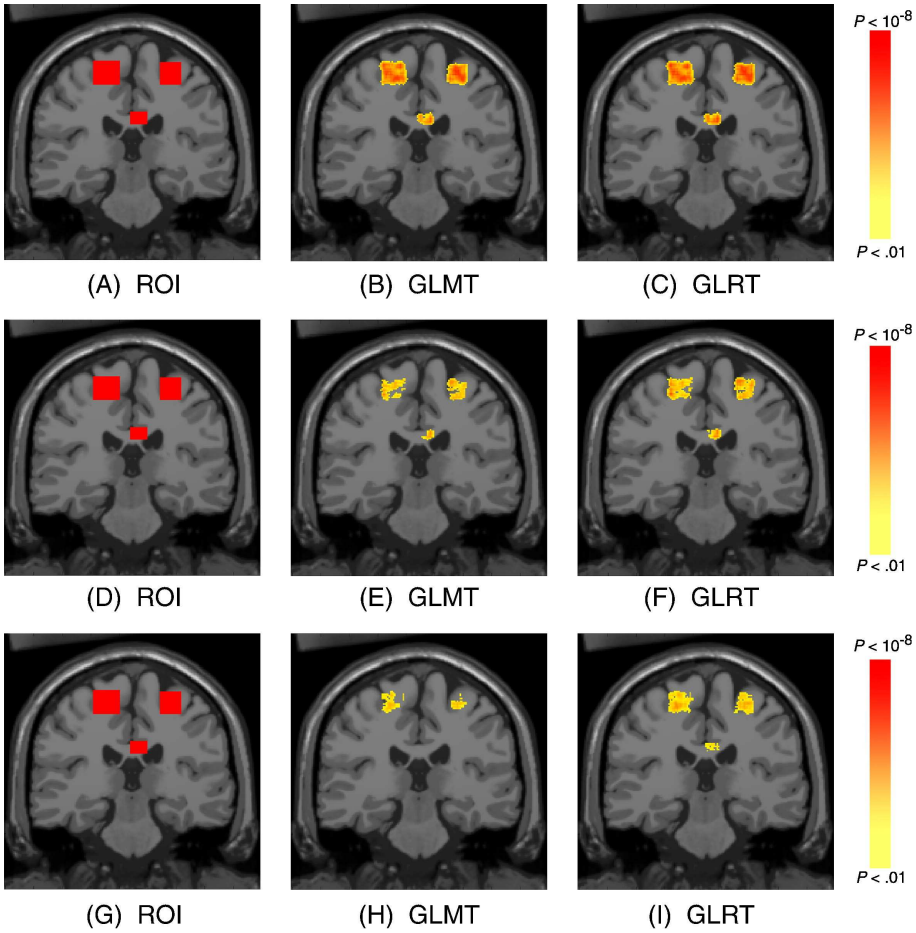

Fig. 4. Activation detection results of the GLMT and the proposed GLRT after clustering. Synthetic MRI images are shown with activations superimposed in color. The first column (A,D,G) shows three regions in which functional activation was simulated. The second column (B,E,H) and third column (C,F,I) show the detection results (in terms of P values) of the GLMT and the proposed GLRT, respectively. Activation detection is done at a false alarm rate of 0.01. This was done for three values of μ, 0.05, 0.075 and 0.10, shown in the first row (A–C), second row (D–F) and third row (G–I), respectively. The corresponding values of σ were 2.5, 4.0 and 5.0.

the simulation results that although the performance of the GLRT (incorporating the Rician distribution of the data) is always better than that of the GLMT (ignoring the non-Gaussian distribution of the data), the difference will no longer be significant for relatively high SNR values (>10). This means that for high SNR values, ignoring the non-Gaussian distribution of the noise in statistical fMRI data analysis is rather harmless. However, the results also show that for low SNR (<10), the GLMT loses its CFAR property and is therefore no longer a reliable test. The GLRT on the other hand will stay CFAR for low values of the SNR (at least for SNR>1).

5. Conclusions

Most statistical fMRI data analyses assume a Gaussian distribution of the data. A common approach is the GLMT, which is in fact a GLRT under the assumption of Gaussian-distributed data. Magnitude fMRI data, however, are characterized by a Rician distribution. In this work, it has been shown that if the SNR of the data is relatively high (>10), ignoring the non-Gaussian distribution of the data hardly affects the performance of the analysis. However, if the SNR is relatively low (<10), not incorporating the exact nature of the data distribution leads to suboptimal test results. In particular, simulation results clearly show that the commonly used GLMT does not have the CFAR property at low values of the SNR and is therefore unreliable. On the other hand, the proposed GLRT for magnitude fMRI data was shown to have the CFAR property even at low values of the SNR.

Acknowledgment

J. Sijbers is a Postdoctoral Fellow of the F.W.O. (National Fund for Scientific Research, Belgium).

References

[1] Lukic AS, Wernick MN, Strother SC. An evaluation of methods for detecting brain activations from functional neuroimages. Artif Intell Med 2002;25(1):69–88.

[2] Gudbjartsson H, Patz S. The Rician distribution of noisy MRI data. Magn Reson Med 1995;34:910–4.

[3] Karlsen OT, Verhagen R, Bovée WM. Parameter estimation from Rician-distributed data sets using a maximum likelihood estimator: application to T_1 and perfusion measurements. Magn Reson Med 1999;41(3):614–23.

[4] Soltanian-Zadeh H, Peck DJ, Hearshen DO, Lajiness-ONeill RR. Model-independent method for fMRI analysis. IEEE Trans Med Imaging 2004;23(3):285–96.

[5] Rowe DB, Logan BR. A complex way to compute fMRI activation. Neuroimage 2004;23(3):1078–92.

[6] Nan FY, Nowak RD. Generalized likelihood ratio detection for fMRI using complex data. IEEE Trans Med Imaging 1999;18(4):320–9.

[7] Rowe DB. Parameter estimation in the magnitude-only and complex-valued fMRI data models. Neuroimage 2005;25:1124–32.

[8] Sijbers J, den Dekker AJ. Generalized likelihood ratio tests for complex fMRI data: a simulation study. IEEE Trans Med Imaging 2005;24(5):604–11.

[9] Friston KJ, Jezzard P, Turner R. Analysis of functional MRI time series. Hum Brain Mapp 1994;1:153–71.

[10] Mood AM, Graybill FA, Boes DC. Introduction to the theory of statistics. 3rd ed. Tokyo: McGraw-Hill; 1974.

[11] Wilks SS. Mathematical statistics. New York: John Wiley and Sons Inc; 1961.

[12] Kay SM. Fundamentals of statistical signal processing, volume II detection theory. Upper Saddle River (New Jersey): Prentice Hall PTR; 1998.

[13] Bonny JM, Renou JP, Zanca M. Optimal measurement of magnitude and phase from MR data. J Magn Reson 1996;113:136–44.

[14] Sijbers J, den Dekker AJ. Maximum likelihood estimation of signal amplitude and noise variance from MR data. Magn Reson Med 2004;51(3):586–94.

[15] van den Bos A. Handbook of measurement science. In: Sydenham PH, editor. Parameter estimation, vol. 1. Chichester (England): Wiley; 1982. p. 331–77 [ch. 8].

[16] Scharf LL, Friedlander B. Matched subspace detectors. IEEE Trans Signal Process 1994;42(8):2146–57.

[17] Ardekani BA, Kershaw J, Kashikura K, Kanno I. Activation detection in functional MRI using subspace modeling and maximum likelihood estimation. IEEE Trans Med Imaging 1999;18(2):246–54.

[18] Press WH, Vettering WT, Teukolsky SA, Flannery BP. Numerical recipes in C. Cambridge: University Press; 1994 [chap. 10].

[19] Collins DL, Zijdenbos AP, Kollokian V, Sled JG, Kabani NJ, Holmes CJ, et al. Design and construction of a realistic digital brain phantom. IEEE Trans Med Imaging 1998;17(3):463–8.

[20] Sijbers J, den Dekker AJ, Raman E, Van Dyck D. Parameter estimation from magnitude MR images. Int J Imaging Syst Technol 1999;10(2):109–14.

[21] Petersson KM, Nichols TE, Poline J-B, Holmes AP. Statistical limitations in functional neuroimaging II: signal detection and statistical inference. Philos Trans R Soc Lond B 1999;354:1261–82.